



Methoxy-substituted 9-aminomethyl-9,10-dihydroanthracene (AMDA) derivatives exhibit differential binding affinities at the 5-HT_{2A} receptor

Gajanan K. Dewkar^a, Srinivas Peddi^a, Philip D. Mosier^a, Bryan L. Roth^b, Richard B. Westkaemper^{a,*}

^a Department of Medicinal Chemistry, School of Pharmacy, Virginia Commonwealth University, 410 N. 12th Street, PO Box 980540, Richmond, VA 23298-0540, USA

^b Departments of Pharmacology and Medicinal Chemistry, Lineberger Cancer Center, Neurosciences Program and NIMH Psychoactive Drug Screening Program, University of North Carolina School of Medicine, Chapel Hill, NC 27599, USA

ARTICLE INFO

Article history:

Received 27 May 2008

Revised 15 August 2008

Accepted 18 August 2008

Available online 22 August 2008

Keywords:

5-HT_{2A}

AMDA

Homology model

ABSTRACT

The effects of methoxy-substitution at the 1-, 2-, 3-, and 4-positions of 9-aminomethyl-9,10-dihydroanthracene (AMDA) on h5-HT_{2A} receptor affinity were determined. Racemic mixtures of these compounds were found to show the following affinity trend: 3-MeO > 4-MeO > 1-MeO ~ 2-MeO. Comparison of the effects of these substitutions, with the aid of computational molecular modeling techniques, suggest that the various positional and stereochemical isomers of the methoxy-substituted AMDA compounds interact differently with the h5-HT_{2A} receptor. It is predicted that for the compounds with higher affinities, the methoxy oxygen atom is able to interact with hydrogen bond-donating sidechains within alternative h5-HT_{2A} receptor binding sites, whereas the lower-affinity isomers lack this ability.

© 2008 Elsevier Ltd. All rights reserved.

The chemical features that are responsible for the potency and efficacy of agents that bind to 5-HT_{2A} receptors, as well as the receptor–ligand interactions responsible for the ligands' observed affinities, have not yet been fully elucidated. Toward that end, we have synthesized and assayed many analogs¹ of the selective² 5-HT_{2A} antagonist³ 9-aminomethyl-9,10-dihydroanthracene (AMDA, **1**). This work in particular builds upon earlier studies¹ of AMDA analogs in which it was shown that substituents of widely varying size and polarity may be placed at the 3-position without a large decrease in 5-HT_{2A} affinity. In order to more completely determine the extent of this apparent steric and/or electrostatic tolerance, and in particular to find AMDA analogs that have a significantly reduced affinity for the 5-HT_{2A} receptor, a series of AMDA analogs that are substituted at varying positions around the AMDA core were synthesized and tested. The methoxy group was chosen a general-purpose 'probe' functional group because of its synthetic flexibility, small size, and amphiphilic nature (i.e., it is able to participate in both polar and non-polar interactions). The results of a systematic study of methoxy-substituted AMDA compounds, and the concomitant effects that these substitutions have upon the compounds' affinity for the human 5-HT_{2A} receptor are reported here.

Radioligand binding data (5-HT_{2A} receptor affinities) were obtained for each of the target compounds (Table 1). Within the methoxy-substituted AMDA series, the affinities varied by more than 180-fold (**4**, $K_i = 7.5$ nM; **3**, $K_i = 1367$ nM). Of all four

positional isomers, only 3-methoxy-AMDA (**4**) showed increased affinity relative to the parent compound AMDA ($K_i = 20$ nM). 4-Methoxy-AMDA (**5**, $K_i = 124$ nM) displayed a modest sixfold decrease in affinity compared to AMDA, while both 1- and 2-methoxy-AMDA (**2**, $K_i = 1158$ nM and **3**, $K_i = 1367$ nM, respectively) were found to have substantially reduced affinity (>50-fold) compared to AMDA.

Previous receptor modeling studies¹ have identified two possible binding sites for 5-HT_{2A} ligands, as shown schematically in Figure 1. Site 1 is flanked primarily by transmembrane helices TM3, TM5, and TM6, and has been proposed as the binding site for agonists,^{4,5} partial agonists,⁶ and antagonists.^{7,8} Site 2 is an alternative binding site and is flanked by TM1, TM2, TM3, and TM7. Ketanserin⁹, a prototypical 5-HT_{2A} antagonist, and similar butyrophenones¹⁰ have been proposed to simultaneously bind in both sites.

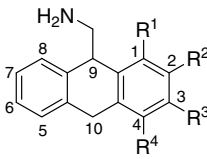
Each compound in Table 1 (with explicit consideration of stereoisomers) was docked into two graphical receptor models representing the agonist-selected Site 1 and the antagonist-selected Site 2 (see Experimental methods). The overall quality of the docked poses was determined using the ChemScore fitness function with visual inspection of the docked solutions, and the top-ranking solution for each isomer was selected (see Supplemental Table S1). In each case, GOLD was able to place the ligand into both Site 1 and Site 2. However, productive hydrogen bonds were formed only for the more potent 3-methoxy-AMDA ((R)-**4** and (S)-**4**) and 4-methoxy-AMDA ((S)-**5**).¹¹ For (R)-**4**, the methoxy oxygen H-bonds with S159^{3,36}, for (S)-**4**, the H-bond donor is S131^{2,61}, and for (S)-**5**, H-bonding occurs with S239^{5,43} (see Fig. 2). In each of these

* Corresponding author. Tel.: +1 804 828 6449; fax: +1 804 828 7625.

E-mail address: rbwestka@vcu.edu (R.B. Westkaemper).

Table 1

Observed binding affinities for AMDA and methoxy-substituted AMDA analogs at the h5-HT_{2A} receptor



Compound	R ¹	R ²	R ³	R ⁴	K _i , nM ^a
1	–H	–H	–H	–H	20
2	–OCH ₃	–H	–H	–H	1158
3	–H	–OCH ₃	–H	–H	1367
4	–H	–H	–OCH ₃	–H	7.5
5	–H	–H	–H	–OCH ₃	124

^a [³H]Ketanserin labeled cloned 5-HT_{2A} sites. Values represent the mean of computer-derived K_i estimates (using GraphPad Prism) of quadruplicate determinations. Standard errors typically range between 15% and 25% of the K_i value.

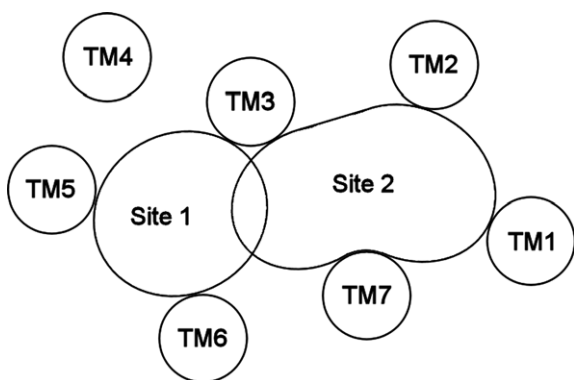


Figure 1. Schematic representation of sterically accessible binding sites (Site 1 and Site 2) within the 5-HT_{2A} receptor.

solutions, the ammonium ion interacts with D155^{3,32} and with other lipophilic/aromatic residues surrounding the AMDA core (see Supplemental Table S2). The current models are consistent with earlier mutagenesis and molecular modeling studies.¹² The fact that both isomers of **4** are able to H-bond with the receptor and both receive a relatively high ChemScore is consistent with its low K_i value. Although there are several hydrogen bond donating sites within the agonist-selected Site 1 (S159^{3,36}, T160^{3,37}, S239^{5,43}, S242^{5,46}, W336^{6,48}, N343^{6,55}) and antagonist-selected Site 2 (S77^{1,35}, T81^{1,39}, S131^{2,61}, W151^{3,28}, S159^{3,36}, S373^{7,46}), our results suggest that 1-methoxy AMDA (**2**) and 2-methoxy-AMDA (**3**) are not able to position themselves within these sites in a way that allows the methoxy group to beneficially interact with them. This in turn is consistent with the significantly reduced affinity of **2** and **3** for h5-HT_{2A}. The binding affinity of the methoxy-AMDA compounds can thus be directly correlated with their ability to H-bond with residues in Site 1 or Site 2.

It should be noted that an alternative explanation for the reduced activity of **2** is the possibility of internal H-bond formation. This would reduce the effectiveness of the amine and the methoxy group to act as an H-bond donor and acceptor, respectively, and could potentially impose a ligand conformation that reduces the complementarity of the ligand to its binding site.

AMDA (**1**) was synthesized as previously described.³ The synthesis of 1-methoxy- (**2**) and 2-methoxy-9-aminomethyl-9,10-dihydroanthracene (**3**) (Scheme 1) was brought about by the 1,4-addition of 2-[(methoxymethoxy)-methyl]phenylmagnesium bromide¹³ to the nitrostyrenes **6a** and **6b**¹⁴ to give substituted 1,1-diary-2-nitroethanes **7a** and **7b**. The MOM-protected benzyl alcohols **7a** and **7b** were deprotected using HCl to give the nitro alcohols **8a**

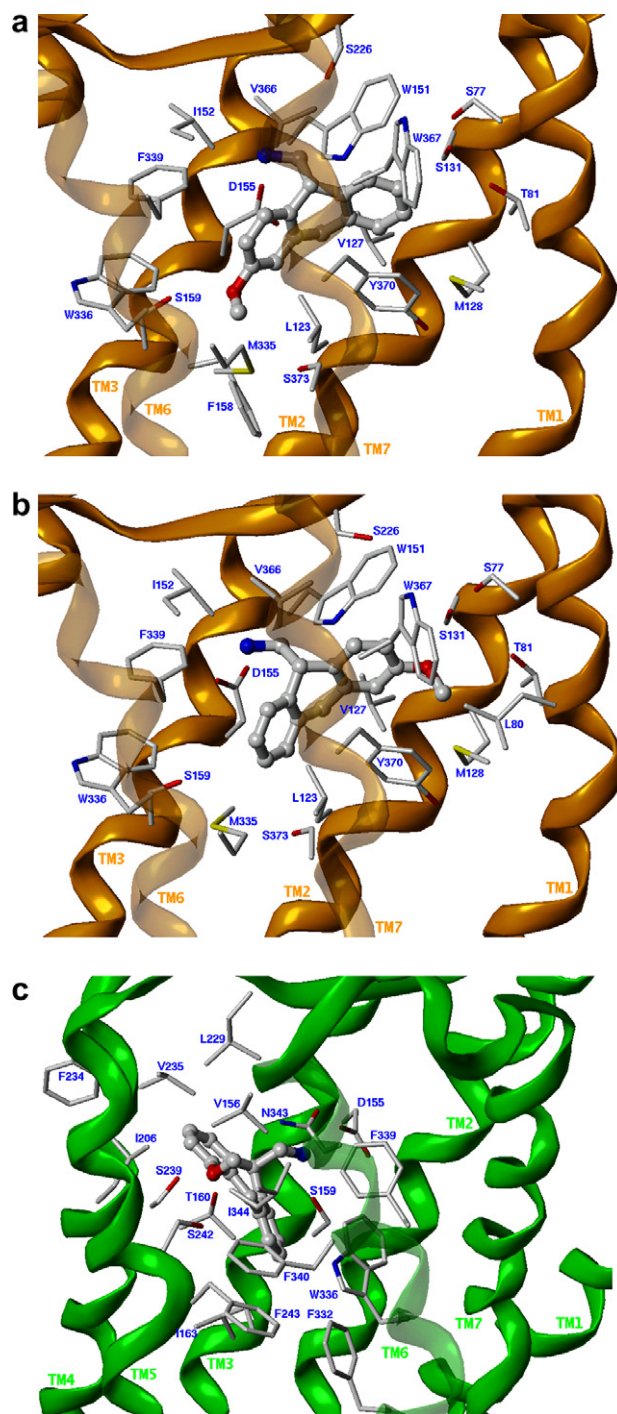
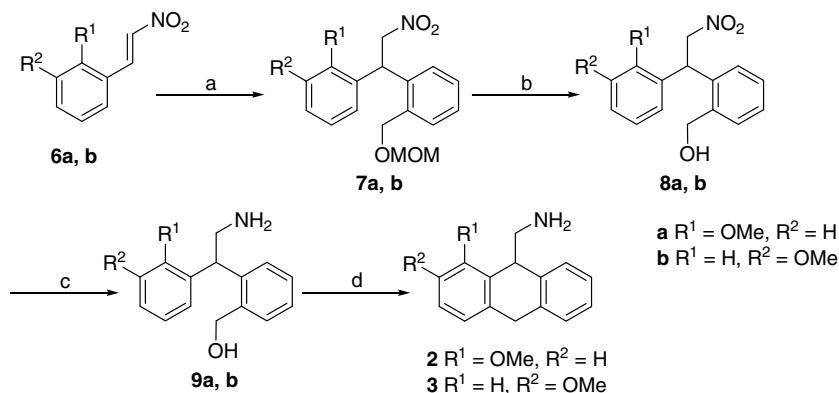
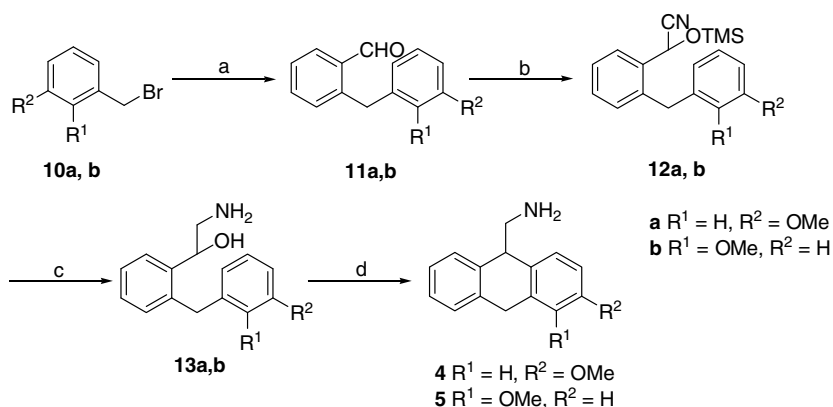


Figure 2. Proposed binding modes of the three MeO-AMDA isomers that exhibit substantial hydrogen-binding interactions with residues within the binding crevice of the h5-HT_{2A} receptor. The receptor backbone for models representing Site 1 (agonist-selected) are indicated with a green ribbon; those representing Site 2 (antagonist-selected) are indicated with an orange ribbon. The sidechains of 5-HT_{2A} residues within 5 Å of the ligand are displayed as capped sticks and the ligand is rendered as a ball-and-stick model. (a) (R)-3-Methoxy-AMDA ((R)-4) in Site 2. (b) (S)-3-Methoxy-AMDA ((S)-4) in Site 2. (c) (S)-4-Methoxy-AMDA ((S)-5) in Site 1.

and **8b**, which were reduced to their respective amines to give amino alcohols **9a** and **9b**. Cyclodehydration of amino alcohols **9a** and **9b** using freshly prepared PPE in CHCl₃ gave the 1- and 2-methoxy substituted AMDAs **2** and **3**, respectively. Synthesis of 3-methoxy- (**4**) and 4-methoxy-9-aminomethyl-9,10-dihydroanthracenes (**5**) (Scheme 2) was brought about by a standard Suzuki cross-coupling



Scheme 1. Reagents and conditions: (a) 1-bromo-2-((methoxymethoxy)methyl)benzene, Mg, I_2 , THF, 65 \rightarrow 0 $^\circ\text{C}$, 12 h; (b) HCl, MeOH, 65 $^\circ\text{C}$, 5 h; (c) H_2 , (50 psi), MeOH, 10% Pd/C, 25 $^\circ\text{C}$, 36 h; (d) PPE, CHCl_3 , reflux, 3 h.



Scheme 2. Reagents and conditions: (a) 2-formylphenylboronic acid, $\text{Pd}(\text{PPh}_3)_4$, Na_2CO_3 , toluene/ethanol (9:1), 100 $^\circ\text{C}$, 3 h; (b) TMSCN, ZnI_2 , CH_2Cl_2 , 65 $^\circ\text{C}$, 4 h; (c) LiAlH_4 , THF, reflux, 12 h; (d) $\text{CH}_3\text{SO}_3\text{H}$, 25 $^\circ\text{C}$, 12 h; PPA, 60 $^\circ\text{C}$, 6 h.

reaction between commercially available 3-methoxybenzyl bromide **10a** or 2-methoxybenzyl bromide **10b**¹⁵ and 2-formylphenylboronic acid to yield 2-(3-methoxybenzyl)benzaldehyde **11a** and 2-(2-methoxybenzyl)benzaldehyde **11b**. Cyanosilylation of the aldehydes **11a** and **11b** using TMSCN gave the corresponding cyano trimethylsilyl ethers **12a** and **12b**, which were reduced with LiAlH_4 to give the respective amino alcohols **13a** and **13b**. Cyclodehydration of amino alcohols **13a** and **13b** using $\text{CH}_3\text{SO}_3\text{H}$ and PPA, respectively, gave the 3-methoxy- and 4-methoxy-substituted AM-DAs **4** and **5**.

The molecular modeling methodology used to generate the h5-HT_{2A} receptor–ligand complex models will be described briefly here, and is discussed in detail elsewhere.¹² To begin, the h5-HT_{2A} receptor sequence was aligned using ClustalX 1.83¹⁶ with a profile of several related class A GPCRs¹⁷ that included bovine rhodopsin. The result was an unambiguous alignment (in the TM helical regions) of the h5-HT_{2A} sequence with that of bovine rhodopsin. Manual modifications were made to the alignment in the region of the second extracellular loop to properly align the cysteine residues of the disulfide linkage. This alignment, along with a file containing the atomic coordinates of bovine rhodopsin ('A' chain of PDB code 1U19), was used as input to the MODELLER software package^{18,19} to generate a population of 100 h5-HT_{2A} homology models, each with a different conformation. For the template rhodopsin structure, all residues within 12 Å of the bound retinal ligand were mutated to alanine to encourage MODELLER to produce structurally diverse receptor conformations. The N- and C-termini were truncated. The third intracellular loop was modeled simply as a poly-Gly chain whose backbone coordinates were taken from the structure of rhodopsin. Each receptor in the

population was subsequently energy-minimized without constraint in SYBYL 7.2 (Tripos Inc., St. Louis, MO) using the Tripos Force Field (TFF) with Gasteiger–Hückel charges, a distance-dependent dielectric constant of 4, a non-bonded interaction cutoff = 8 Å, and were terminated at an energy gradient of 0.05 kcal/(mol Å). The automated docking program GOLD^{20,21} version 3.01 (Cambridge Crystallographic Data Centre, Cambridge, UK) was then used to dock a potent 5-HT_{2A} agonist (1-(2,5-dimethoxy-4-bromophenyl)-2-aminopropane; DOB) and a potent antagonist (ketanserin) into each of the 100 receptor models. Based on the fitness scores and quality of the docked poses, one receptor model was selected to represent the agonist binding site (Site 1 in Fig. 1) and a second model was selected to represent an additional antagonist binding site (Site 2 in Fig. 1). After a small amount of conformational refinement and checks for stereochemical integrity, the two receptor models were saved and used for subsequent docking exercises.

Ligand molecules were sketched in using SYBYL and energy-minimized using the same method and parameters as were used for the receptor models. Basic amines were protonated to form ammonium ions. Ligand chirality was treated explicitly, with each isomer sketched, energy-minimized and saved as a separate structure file. GOLD was then used to dock each ligand structure into each of the two selected receptor models. The parameter set defined by the 'standard default settings' option was used in conjunction with a protein H-bond constraint (default settings) that biased the docked solutions in favor of those in which the ligand ammonium ion interacted with the conserved D155^{3,32}. Ten genetic algorithm (GA) runs were performed for each ligand at both Site 1 and Site 2. Short molecular dynamics (MD) simulations were then carried out to enable the receptor–ligand complex to sample alterna-

tive locally accessible low-energy states in order to improve the binding free energy, and to simultaneously increase the degree of receptor–ligand complementarity. The MD simulations were run at 300 K for 100 ps using the TFF with assigned Gasteiger–Hückel charges, a distance-dependent dielectric constant = 4.0 and a non-bonded interaction cutoff of 8.0 Å. To maintain the structural integrity of the receptor–ligand complexes during the MD run, an aggregate was defined that constrained the atoms of all residues greater than 8.0 Å from the GOLD-docked solution to their starting coordinates. The receptor–ligand complexes were then subjected to a final energy minimization step using the same parameters as shown above. All molecular modeling was performed on MIPS R14K- and R16K-based IRIX 6.5 Silicon Graphics Fuel and Tezro workstations.

Binding assays and data analysis were performed through the NIMH Psychoactive Drug Screening Program (PDSP). The 5HT_{2A} competitive binding assay employs [³H]ketanserin (a 5-HT_{2A} antagonist) as the radioligand. Binding data were analyzed using Prism (GraphPad Software, Inc., San Diego, CA). Details of the binding assay protocol may be found at the PDSP home page, <http://pdsp.med.unc.edu>.

Acknowledgments

This work was supported by United States Public Health Service Grant R01-MH57969 (RBW), R01-MH57635 (BLR), K02-MH01366 (BLR) and R01-MH61887 (BLR), U19-MH82441 (BLR) and the NIMH Psychoactive Drug Screening Program (BLR).

Supplementary data

Supplementary data associated with this article can be found, in the online version, at [doi:10.1016/j.bmcl.2008.08.059](https://doi.org/10.1016/j.bmcl.2008.08.059).

References and notes

- Westkaemper, R. B.; Glennon, R. A. *Curr. Top. Med. Chem.* **2002**, *2*, 575.
- Runyon, S. P.; Savage, J. E.; Taroua, M.; Roth, B. L.; Glennon, R. A.; Westkaemper, R. B. *Bioorg. Med. Chem. Lett.* **2001**, *11*, 655.
- Westkaemper, R. B.; Runyon, S. P.; Bondarev, M. L.; Savage, J. E.; Roth, B. L.; Glennon, R. A. *Eur. J. Pharmacol.* **1999**, *380*, R5.
- Braden, M. R.; Parrish, J. C.; Naylor, J. C.; Nichols, D. E. *Mol. Pharmacol.* **2006**, *70*, 1956.
- Shapiro, D. A.; Kristiansen, K.; Kroeze, W. K.; Roth, B. L. *Mol. Pharmacol.* **2000**, *58*, 877.
- Chambers, J. J.; Nichols, D. E. *J. Comput.-Aided Mol. Des.* **2002**, *16*, 511.
- Muntasir, H. A.; Rashid, M.; Komiyama, T.; Kawakami, J.; Nagatomo, T. *J. Pharmacol. Sci.* **2006**, *102*, 55.
- Westkaemper, R. B.; Runyon, S. P.; Savage, J. E.; Roth, B. L.; Glennon, R. A. *Bioorg. Med. Chem. Lett.* **2001**, *11*, 563.
- Dezi, C.; Brea, J.; Alvarado, M.; Raviña, E.; Masaguer, C. F.; Loza, M. I.; Sanz, F.; Pastor, M. *J. Med. Chem.* **2007**, *50*, 3242.
- Brea, J.; Castro, M.; Loza, M. I.; Masaguer, C. F.; Raviña, E.; Dezi, C.; Pastor, M.; Sanz, F.; Cabrero-Castel, A.; Galán-Rodríguez, B.; Fernández-Espejo, E.; Maldonado, R.; Robledo, P. *Neuropharmacology* **2006**, *51*, 251.
- Individual amino acid residues of the receptor are identified by the traditional residue identifier indicating the residue's position in the primary amino acid sequence, followed by the general Ballesteros–Weinstein GPCR residue identifier as a superscript. See Ballesteros, J. A.; Weinstein, H. *Methods Neurosci.* **1995**, *25*, 366.
- Runyon, S. P.; Savage, J. E.; Mosier, P. D.; Roth, B. L.; Glennon, R. A.; Westkaemper, R. B. *J. Med. Chem.*, submitted for publication.
- Ashwood, M. S.; Bell, L. A.; Houghton, P. G.; Wright, S. H. *Synthesis* **1988**, 1988, 379.
- Furniss, B. S.; Hannaford, A. J.; Smith, P. W. G.; Tatchell, A. R. *Vogel's Textbook of Practical Organic Chemistry*; Longman: Harlow, 1989.
- Dijks, F. A.; Grove, S. J. A.; Carlyle, I. C.; Thorn, S. N.; Rae, D. R.; Ruigt, G. S. F.; Leysen, D. International Patent WO/1999/18941, 1999, 50 pp.
- Chenna, R.; Sugawara, H.; Koike, T.; Lopez, R.; Gibson, T. J.; Higgins, D. G.; Thompson, J. D. *Nucleic Acids Res.* **2003**, *31*, 3497.
- Bissantz, C.; Bernard, P.; Hilbert, M.; Rognan, D. *Proteins* **2003**, *50*, 5.
- Fiser, A.; Šali, A. In *Methods in Enzymology: Macromolecular Crystallography: Part D*; Carter, C. W. J., Sweet, R. M., Eds., 2003; Vol. 374, p. 461.
- Šali, A.; Blundell, T. L. *J. Mol. Biol.* **1993**, *234*, 779.
- Jones, G.; Willett, P.; Glen, R. C. *J. Mol. Biol.* **1995**, *245*, 43.
- Jones, G.; Willett, P.; Glen, R. C.; Leach, A. R.; Taylor, R. J. *Mol. Biol.* **1997**, *267*, 727.